17 Lecture, 28 October 1999

17.1 Seeing

The refractive index of air is close to unity, but not close enough to spare astronomers from one of their most persistent adversaries, turbulence. Energy from solar and local sources is constantly pumped into the atmosphere between telescope and celestial object, changing the temperature and pressure of the air where it is absorbed, in a manner that leads to a variety of fluid instabilities. The development over time of the instabilities gives rise to fluctuations in the density of air – and therefore in the refractive index of the atmosphere – and motions of these locally overdense or underdense air. We feel and see the results in the form of wind, atmospheric turbulence, and the twinkling of stars; the latter results in a blurring of the images of the stars, and is the effect to which astronomers refer as *seeing*. "Good seeing" is when the stars twinkle very little; "bad seeing" is when they twinkle a lot. Seeing is of course much more easily noticed when looking through a telescope. The best observing sites in the world usually have seeing, expressed as the FWHM of stellar images at visible wavelengths, in the 0.5-1 arcsec range.

Let us qualitatively explore the influence of randomly-distributed refractive-index fluctuations on images of point-like astronomical objects. Consider a plane wavefront, incident on axis for some telescope, that passes through a turbulent layer of the atmosphere as in Figure 17.1. Pieces of the wavefront that encounter index fluctuations get their curvature changed as a result, since the action of a fluctuation will be akin to that of a weak lens. By the time the wavefront reaches the telescope it will have been distorted with small wrinkles and tilts. Rays of light are perpendicular to wavefronts, so there is a nonzero spread among incidence angles of rays, and a corresponding blur circle in the focal plane. Parts of the wavefront with a given slope correspond to rays of a certain incidence angle, that will all focus to a certain place in the focal plane. Three distinct features of the transmitted waveform are worth specific mention. First, there is generally an overall slope to the wavefront that is different from the initial one. Thus the centroid of the blur pattern does not lie at the spot in the focal plane at which the light originally was aimed. This slope will of course change with time, so the centroid of the focal-plane image will seem to dance around.

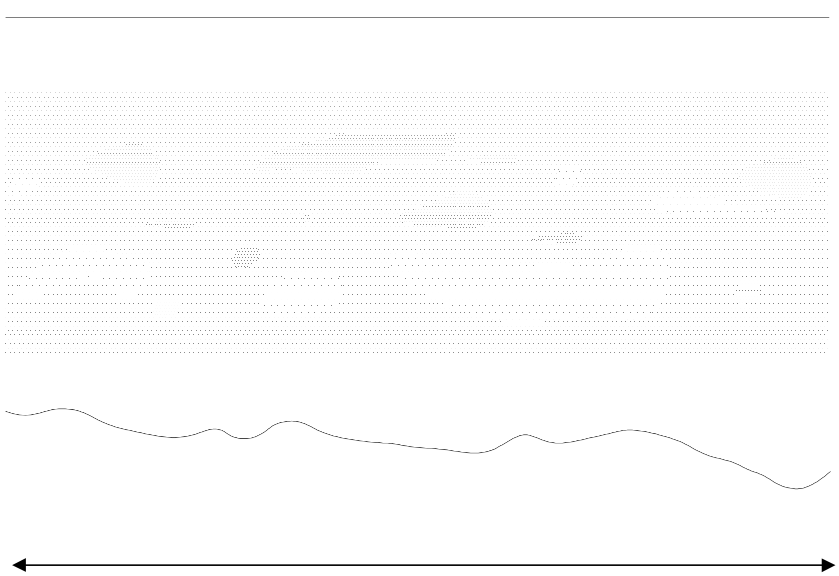

Figure 17.1: schematic diagram of refractive-index fluctuations in the atmosphere, and the effects on initially plane wavefronts as they propagate.

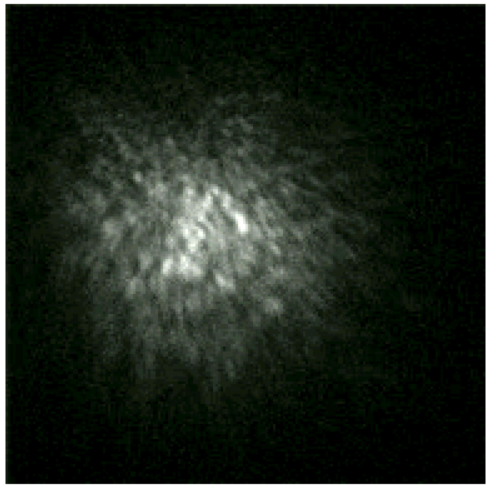

Figure 17.2: short (25 ms) exposure image of the binary star γ Per (0.2″ separation) at λ = 5700 Å with the 4.2 m William Herschel Telescope (Nick Wooder, Imperial College). For an MPEG movie made of 250 consecutive 25 ms exposures of γ Per, see http://op.ph.ic.ac.uk/speckle/movies.html.

Second, there are many wavefront parts with same slope, spread over telescope mirror in projection. These will lead to distinct spots of essentially telescope-diffraction-limited size, called *speckles*, that are randomly placed in the focal plane. As the refractive-index fluctuations do, speckles move around, and come and go, with time. Finally, there are small scale, high-curvature wavefront distortions. If the curvature is high enough the corresponding rays are significantly defocused, compared to the nominal focal plane. These rays are distributed widely and relatively smoothly over the blur circle. All three features appear in the very short-exposure stellar image in Figure 17.2. Most interesting astronomical observations involve long exposures, for which the centroid motion and churning-about of the speckles and defocussed light produce a symmetrical blur with a Gaussian radial brightness dependence called the *seeing disk.*

Three parameters are often used to characterize seeing: the *Fried parameter* r_0, the time scale t_0 on which images change significantly due to seeing, and the *isoplanatic angle* θ_{IP}.

The Fried parameter is the typical diameter of refractive-index fluctuations. In terms of the Fried parameter the FWHM of the seeing disk turns out to be about

$$\Delta\theta_{\mathrm{seeing}} = 1.2\lambda/r_0 \quad , \tag{17.1}$$

which rather easily exceeds the FWHM of the central peak of the Airy pattern, $\Delta\theta_{\mathrm{diffraction}} = 1.2\lambda/D$: the Fried parameter is seen to vary with site and weather conditions roughly in the range 3-30 cm at visible wavelengths. Thus, without correction for seeing, the world's largest telescopes have no better angular resolution than a humble $D \approx r_0 \approx 10$ cm telescope used at the same site. (Of course, the large telescopes can detect much fainter sources than the small one; resolution isn't everything.) Since the number of speckles is given roughly by how many index fluctuations there are in front of the telescope, the Fried parameter gives also an estimate for the number of speckles in the focal plane, as the ratio of telescope area to that of the typical index fluctuation,

$$N \approx D^2/r_0^2 \quad . \tag{17.2}$$

It is predicted from the Kolmogorov theory of turbulence, and the known dispersion of air, that the Fried parameter varies with wavelength as $r_0 \propto \lambda^{6/5}$. Thus the FWHM diameter of the seeing disk should get smaller gradually as wavelength increases, as $\Delta\theta_{\text{seeing}} \propto \lambda^{-1/5}$; this has been verified experimentally.

Homework problem 17.1. At Mauna Kea the seeing at visible ($\lambda = 0.55\ \mu\text{m}$) wavelengths is about 0.5 arcsec about half of the time. The big optical telescopes on this mountain, 3-10 m in diameter, are used at visible wavelengths, to be sure, but also in the atmospheric windows in the infrared (e.g. 2.2, 10 and 20 μm). There are also two submillimeter telescopes, 10 and 15 m in diameter, used most frequently at 350 and 850 μm, and one element of the VLBA, 25 m diameter, operating typically at a wavelength of 2 cm. Compare the FWHM sizes of the seeing disk and the Airy disk for these telescopes at their operating wavelengths. At what wavelengths is the angular resolution of each telescope (assumed geometrically perfect) determined by diffraction? By seeing?

Homework problem 17.2. The dependence of focal-plane intensity on radial distance is adequately represented by a Gaussian function in both the seeing disk and the Airy disk, with FWHM times plate scale given by $\Delta\theta_{\text{seeing}}$ and $\Delta\theta_{\text{diffraction}}$. The combination of seeing and diffraction is described by the convolution of those two functions.

a. Show that stellar images made with telescopes that lack significant aberrations have intensity as a function of radial distance described by a Gaussian with FWHM given by $\Delta\theta = \sqrt{\Delta\theta_{\text{seeing}}^2 + \Delta\theta_{\text{diffraction}}^2}$. (*Hint*: consult homework problem 13.1, and use the convolution theorem.)

b. Plot the FWHM of a stellar image as a function of wavelength from 0.2 to 20 μm, for a 10 m diameter telescope with 0.5 arcsec seeing at $\lambda = 0.55\ \mu\text{m}$. At what wavelength is the angular resolution of such a telescope at its best?

The time scale for a significant change the arrangement of index fluctuations is most often determined by the speed of the wind, rather than by the seething, boiling-like motions to which these air bubbles are also subject. If the wind blows at speed $v = 500$ cm s^{-1} (11 mph), an index fluctuation of typical size moves by its own diameter in $t_0 = r_0/v = 20$ ms. Thus to make an image of the pattern of speckles in sharp detail, or to make an optical correction toward the amelioration of seeing, one must act quickly, with exposure or reaction times in the few to few tens of milliseconds.

Plane waves originating in two point objects very close together on the sky can be considered to traverse essentially the same pattern of refractive-index fluctuations on their way into the optics; those from more distant objects pass through a different set of cells. The reference angle by which we judge close and far is the isoplanatic angle, which can be estimated as follows. Suppose that the index fluctuations lie predominantly at elevation h above the telescope; then the incidence angle for which the turbulence pattern is shifted by r_0 from the on-axis case – losing some of the fluctuations on the edge, passing through others not encountered by the on-axis wavefronts – gives an angle r_0/h. Detailed calculations are in agreement with this estimate: the isoplanatic angle, given by such calculations as

$$\theta_{\text{IP}} \cong \frac{r_0}{3h} \quad , \tag{17.3}$$

defines a solid angle within which the details of seeing – centroid location, pattern of speckles, and so forth – are the same throughout. This solid angle is called the *isoplanatic patch*. Its significance is that if the seeing is corrected for one point object in the manners described below, that same correction will also remove the seeing very well for all other objects within θ_{IP} of that point object. Direct measurements of the isoplanatic angle on telescopes for which local sources of air turbulence have been carefully eliminated tend to give $\theta_{IP} \approx 5-10''$ at visible wavelengths, which indicates that the air that provides most of the seeing lies 1-2 km above each observatory.

17.2 Adaptive-optical correction of seeing

The best way to eliminate seeing is to remove the observatory from the atmosphere, and this of course is how it was done with the Hubble Space Telescope. The next best way is somehow to correct the image, or better yet the incident wavefront. Correction of the image by a technique known as *speckle interferometry* has been used for a couple of decades. With speckle interferometry it is possible to improve angular resolution dramatically, and even, at near infrared wavelengths, to achieve diffraction-limited resolution on large telescopes. However, the sensitivity obtained in this technique is characterized by the signal-to-noise ratio in a speckle. We have seen that exposure times must be very short in order to see individual speckles, and that each speckle contains only a small fraction of the total power collected by the telescope from a point object. Obviously it would be easier to detect a point source of light if all of its power were concentrated in one diffraction-limited spot, and if very long exposures could be made. Thus a substantial penalty in sensitivity must be paid to use speckle interferometry; it turns out to be useful only on fairly bright astronomical objects.

To enable concentration of light from a point object into a (hopefully diffraction-limited) patch much smaller than the seeing disk, and to enable long exposure times, the wavefront must be corrected in real time before it gets detected. This is the task of *adaptive optics*. A typical adaptive-optical seeing corrector is illustrated in Figure 17.3. It consists mainly of a *wavefront corrector* system of rapidly tiltable and deformable mirrors, that can change the shape of the incident wavefront; a *wavefront sensor*, to tell the corrector what to do; and a point-like object in the same isoplanatic patch as the object whose image is

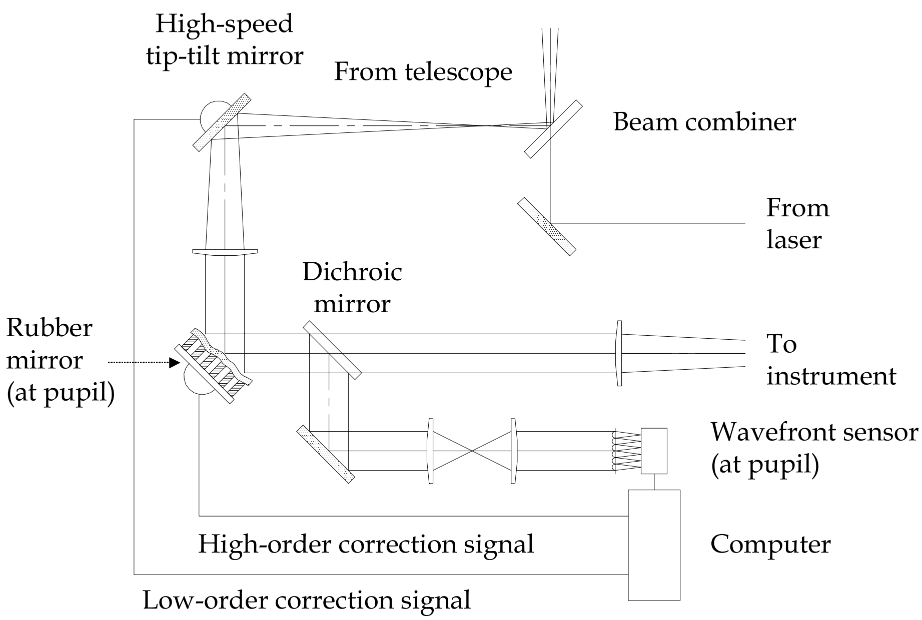

Figure 17.3: schematic diagram of an adaptive-optics corrector system with a laser guide star.

under observation. The point-like object needs to be bright enough to be detected very visibly in an exposure time t_0 or shorter. This object is called the *reference* or *guide star*; it provides wavefronts that can safely be assumed to be planar before they encounter Earth's atmosphere. By splitting off a small fraction of the light and using it in a measurement of this star's wavefronts – specifically, the curvature or phase lag at each point in the wavefronts – one can determine the correction necessary to restore the light from this object to its original plane-wave state. The corrections are applied to the star's wavefronts, and to the light from every other object in the field of view, by the system of tilting and deformable mirrors. The vast bulk of the now-corrected light can continuously be transmitted to an instrument that can measure an image of the field with no restrictions on its exposure time. Everything in the image that lies within an isoplanatic angle of the guide star would thus appear sharper – the effects of seeing are at least partially, sometimes completely, removed.

At the heart of an adaptive-optics system lie the wavefront corrector and sensor. The corrector mirrors have to be able to undo all of the deviations the wavefront underwent while passing through the atmosphere. Usually the overall slope of the reference wavefront, and resulting image centroid motion, is removed with a single mirror that is moved at high speeds in rotation about the *x*- and *y*-axes perpendicular to the optical axis. This part of the system is called a *tip-tilt* corrector. This correction alone can improve images dramatically, especially at infrared wavelengths where the number of speckles is small. An example of the improvement in angular resolution and in the amount of light concentrated in the center of a stellar image is shown in Figure 17.4.

There are several methods currently in use for design of the other elements of an adaptive-optics system; in the following we will describe one with the most popular, and conceptually the simplest, wavefront sensor, called a *Shack-Hartmann sensor*. The setup is illustrated in Figure 17.3. The wavefront corrector and sensor lie at pupils, where ideally the wavefronts from an on-axis point object would be planar and perpendicular to the optical axis. At these pupils the wavefront is separated into many subregions for sensing and correction. To each sensor subregion corresponds one distinct region on the corrector mirror. The distinct regions of the corrector mirror can be adjusted in position – tip, tilt and focus – independently of each other, either making the mirror of many contiguous segments or by using a

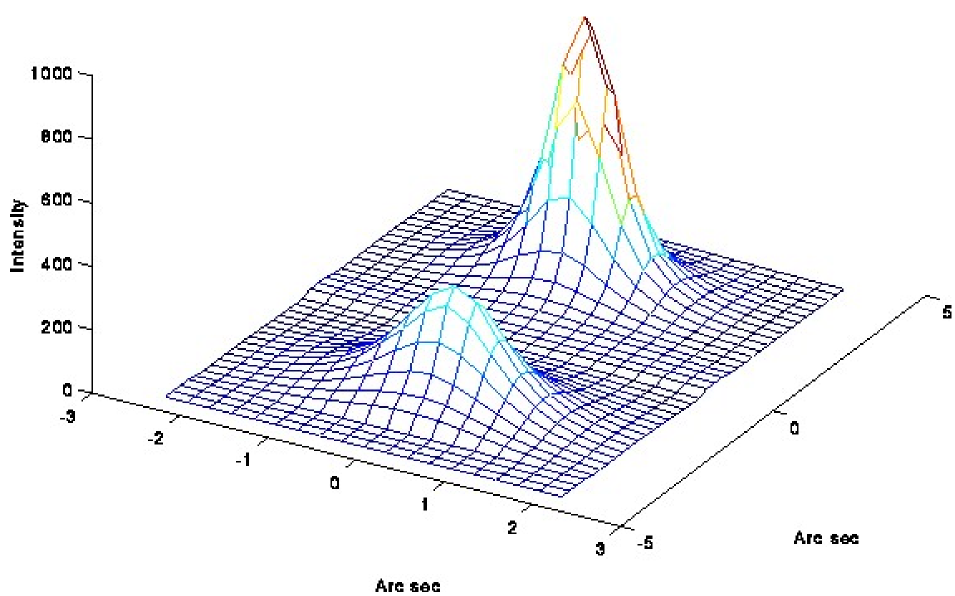

Figure 17.4: Intensity in an image of the star HR 5304 as a function of focal-plane position, observed without (lower) and with (upper) a tip-tilt corrector. (Nick Wooder, Imperial College)

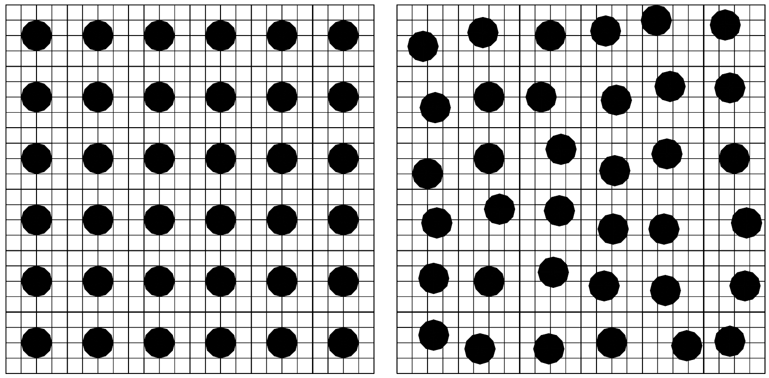

Figure 17.5: schematic diagram of a Shack-Hartmann wavefront-sensor focal plane image, corrected or ideal (left) or distorted and in need of correction (right). The black spots represent guide-star images, the grid pattern the pixels of the wavefront sensor's focal-plane detector array, and the bold grid pattern the boundaries of the cells corresponding to segments of the wavefront corrector's rubber mirror.

flexible, deformable optic; a popular and picturesque name for the latter option is *rubber mirror*. Each of the subregions of the sensor pupil is occupied by a small, short focal-length camera lens. A fast, imaging detector array lies at the common focal plane of the "lenslets." If the guide star's wavefront were planar and on axis, the image seen by this detector array would consist of an array of stellar images, one for each lenslet, each centered in its "cell" of the focal plane. If the images are not centered *on the average*, correction signals are sent to the tip-tilt mirror to steer the average of the guide-star positions back to the cell centers. If after this correction there are individual images that do not lie at their cell centers, correction signals are sent to the positioners of the corresponding regions of the rubber mirror. In each case the correction signal is an electronic instruction to move in the direction that would move the relevant image back toward center, at a rate proportional to the distance of the stellar image from its proper location. In this way each image would "seek" its center and stay there under frequent correction. The process repeats – the system is updated – every $\Delta t \le t_0$. The accuracy of the correction depends principally upon how finely the wavefront sensor and corrector sample the pupil.

For adaptive optics to work, there must be a bright guide star close in projection to the center of the object under study. As you know, nature isn't under our complete control, and a *natural* guide star isn't always available. Considering the small size of the isoplanatic angle, we could find it surprising that natural guide stars are *ever* available – but it turns out that there are a few classes of objects of great current interest, like galactic nuclei, young stellar objects, and compact stellar clusters, for which a reference star is thoughtfully, and centrally, provided. An example of adaptive-optical seeing correction in the center of a Seyfert galaxy, NGC 7469, is shown in Figure 17.6.

For other kinds of objects, and for objects larger than the isoplanatic patch which we nevertheless wish to study at high resolution, a clever technique is employed for creation of an *artificial* guide star in the center of the telescope's field of view. The reference object so obtained is called a *laser guide star.* Two methods are currently in use to produce laser guide stars. About 90 km above Earth's surface is found a rarified layer of air in which a trace of sodium vapor exists, predominantly in neutral atomic form. Sodium has two very strong absorptions, the *D* lines, in the yellow part of the spectrum at λ = 0.58959 and 0.58900 μm. Powerful dye lasers are available that can be tuned to one or other of these wavelengths. If such a laser is pointed out the telescope along the line of sight as in Figure 17.3, focussed at altitude 90 km, the laser light is absorbed and resonantly scattered by the Na I layer. Alternatively, a powerful laser can be focussed at a somewhat lower altitude (20-40 km) and produce an artificial star from the backward scattering of light from molecules in the air. (This adaptation is actually the original, and is called a

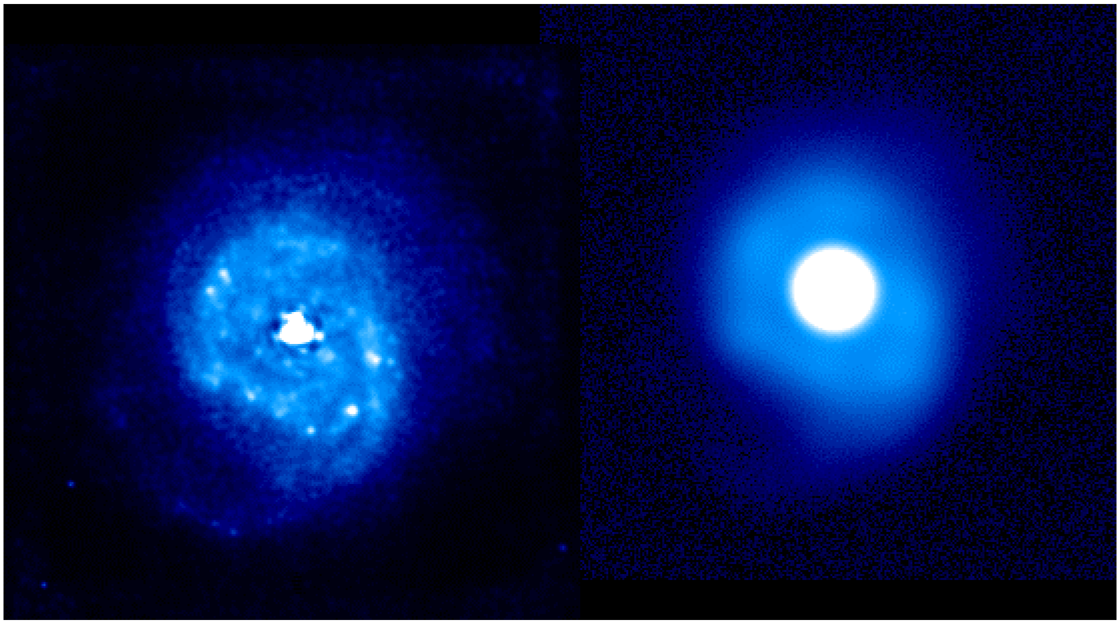

Figure 17.6: the Seyfert 1 galaxy NGC 7469, observed in the near infrared with (left) and without (right) an AO wavefront corrector, on the 3.8 m Canada-France-Hawaii telescope. The galaxy's unresolved nucleus (V= 13.5) served as the guide star. (CFHT)

Rayleigh beacon by its inventors). Either way, a point object is created well into the telescope's far field and well above the bulk of the atmospheric layers in which turbulence is produced. It appears below as a point-like object at the laser's wavelength, in the center of the field of view. The dichroic beamsplitter need only take a "notch" at the laser's wavelength out of the spectrum transmitted to the instrument.

Adaptive-optical correctors with laser guide stars, and about 1000 elements in the wavefront sensor and corrector, represent the state of the art of high-resolution imaging at visible and infrared wavelengths. Diffraction-limited imaging is now achieved routinely at λ = 2.2 μm at the 10 m Keck telescopes on Mauna Kea, and at 0.85 μm on a 3.5 m telescope by the originators of the laser guide star technique.* Some results by the latter group are shown in Figure 17.7 and Figure 17.8, and demonstrate the tremendous improvement in angular resolution and sensitivity given by adaptive optics.

---

* The adaptive-optical imaging group at the US Air Force Research Laboratory's Starfire Optical Range, Robert Fugate and his collaborators, invented and were the first to demonstrate a corrector with a laser guide star (or, to use their term, a Rayleigh beacon). Their work was classified secret, however, and remained so for a while even after the technique was independently developed and demonstrated five years later by non-military astronomers (Thompson and Gardner 1987, *Nature* **328**, 229).

This is one of the better examples of a recent astronomical breakthrough led by scientists funded by the US Department of Defense, whose work was initially carried out in secrecy. We will encounter others this semester when we discuss visible and infrared detector arrays; most readers will also have heard of the most famous instance, the discovery of γ-ray bursters. It is worth keeping these achievements in mind, because academic scientists often commit the injustice of claiming that military research is expensive, inefficient, parasitic and irrelevant. It can be expensive, but it is not noticeably less efficient than research in academe or the national laboratories, and it is certainly neither parasitic nor irrelevant.

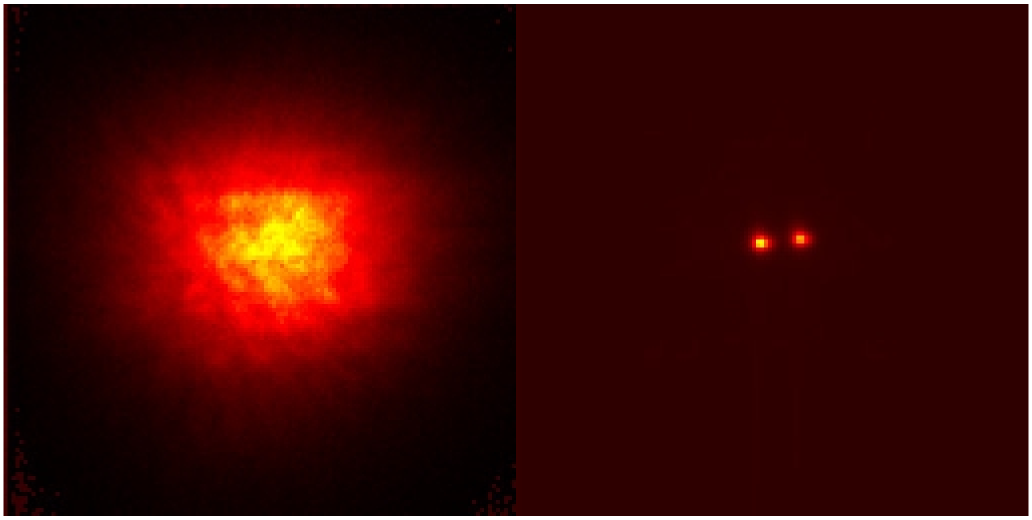

Figure 17.7: Binary star κ Peg (0.3″ separation), observed at λ = 8500 Å without (left) and with (right) a 756-element adaptive-optical corrector and laser guide star (Starfire Optical Range 3.5 m telescope; USAFRL). The brightness scale is different for these two images, but see Figure 17.8 below. The sizes of the corrected stellar images are consistent with the diffraction limit.

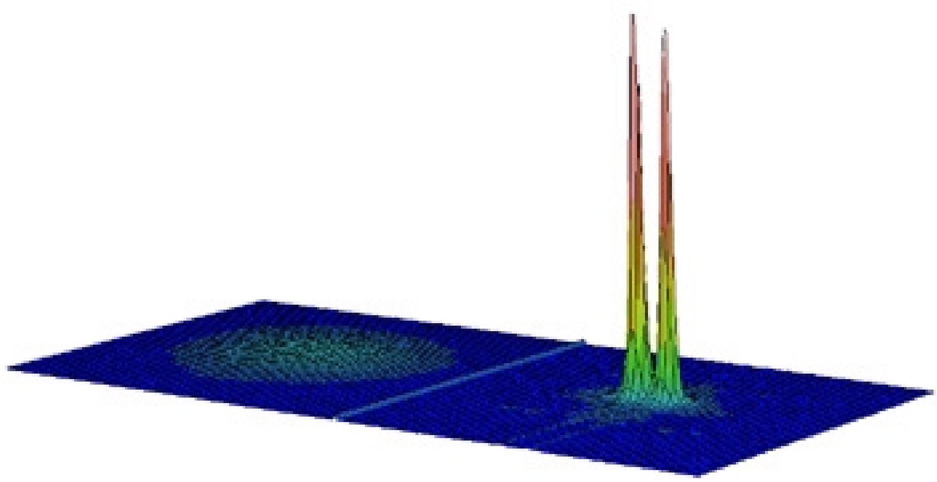

Figure 17.8: The images of κ Peg from Figure 17.7, with detected intensity plotted on the same scale in the third dimension. Note the tremendous increase in the concentrated power in the corrected image.